

Journal of Visualized Experiments

Three-dimensional Characterization of Interorganelle Contact Sites in Hepatocytes using Serial Section Electron Microscopy --Manuscript Draft--

Article Type:	Invited Methods Collection - JoVE Produced Video
Manuscript Number:	JoVE63496R2
Full Title:	Three-dimensional Characterization of Interorganelle Contact Sites in Hepatocytes using Serial Section Electron Microscopy
Corresponding Author:	Jemima Burden LMCB: MRC Laboratory for Molecular Cell Biology London, London UNITED KINGDOM
Corresponding Author's Institution:	LMCB: MRC Laboratory for Molecular Cell Biology
Corresponding Author E-Mail:	j.burden@ucl.ac.uk
Order of Authors:	Jemima Burden Gary Chung Paul Gissen Christopher Stefan
Additional Information:	
Question	Response
Please specify the section of the submitted manuscript.	Biology
Please indicate whether this article will be Standard Access or Open Access.	Standard Access (\$1400)
Please indicate the city, state/province, and country where this article will be filmed . Please do not use abbreviations.	London, WC1E 6BT, UK
Please confirm that you have read and agree to the terms and conditions of the author license agreement that applies below:	I agree to the UK Author License Agreement (for UK authors only)
Please confirm that you have read and agree to the terms and conditions of the video release that applies below:	I agree to the Video Release
Please provide any comments to the journal here.	

TITLE:

Three-dimensional Characterization of Interorganelle Contact Sites in Hepatocytes Using Serial Section Electron Microscopy

AUTHORS AND AFFILIATIONS:

Gary Hong Chun Chung¹, Paul Gissen^{1,2}, Christopher J. Stefan¹, Jemima J. Burden¹

¹MRC Laboratory for Molecular Cell Biology, University College London, Gower Street, London WC1E 6BT, UK

²NIHR Great Ormond Street Hospital Biomedical Research Centre, University College London, Ormond Street, London, WC1N 1EH, UK

Email addresses of co-authors:

Gary Hong Chun Chung (gary.chung@ucl.ac.uk)

Paul Gissen (p.gissen@ucl.ac.uk)

Christopher J. Stefan (c.stefan@ucl.ac.uk)

Corresponding author:

Jemima J. Burden (j.burden@ucl.ac.uk)

SUMMARY:

A simple and comprehensive protocol to acquire three-dimensional details of membrane contact sites between organelles in hepatocytes from the liver or cells in other tissues.

ABSTRACT:

Transmission electron microscopy has been long considered to be the gold standard for the visualization of cellular ultrastructure. However, analysis is often limited to two dimensions, hampering the ability to fully describe the three-dimensional (3D) ultrastructure and functional relationship between organelles. Volume electron microscopy (vEM) describes a collection of techniques that enable the interrogation of cellular ultrastructure in 3D at mesoscale, microscale, and nanoscale resolutions.

This protocol provides an accessible and robust method to acquire vEM data using serial section transmission EM (TEM) and covers the technical aspects of sample processing through to digital 3D reconstruction in a single, straightforward workflow. To demonstrate the usefulness of this technique, the 3D ultrastructural relationship between the endoplasmic reticulum and mitochondria and their contact sites in liver hepatocytes is presented. Interorganelle contacts serve vital roles in the transfer of ions, lipids, nutrients, and other small molecules between organelles. However, despite their initial discovery in hepatocytes, there is still much to learn about their physical features, dynamics, and functions.

Interorganelle contacts can display a range of morphologies, varying in the proximity of the two organelles to one another (typically ~10–30 nm) and the extent of the contact site (from punctate contacts to larger 3D cisternal-like contacts). The examination of close contacts requires high-resolution imaging, and serial section TEM is well suited to visualize the 3D ultrastructural of interorganelle contacts during hepatocyte differentiation, as well as alterations in hepatocyte architecture associated with metabolic diseases.

INTRODUCTION:

Since their invention in the 1930s, electron microscopes have allowed researchers to visualize the structural components of cells and tissues^{1,2}. Most investigations have provided 2D information, as building 3D models requires painstaking serial section collection, manual photography, negative processing, manual tracing, and the creation and assembly of 3D models from sheets of glass, plastic, or Styrofoam^{3,4}. Almost 70 years later, there have been considerable advances in numerous aspects of the process, from microscope performance, serial section collection, automated digital imaging, sophisticated software and hardware for 3D reconstruction, visualization, and analysis to alternative approaches for what is now collectively termed vEM. These vEM techniques are generally considered to provide 3D ultrastructural information at nanometer resolutions across micron scales and encompass transmission electron microscopy (TEM) and newer scanning electron microscopy (SEM) techniques; see reviews⁵⁻⁸.

For example, focused ion beam SEM (FIB-SEM) uses a focused ion beam inside an SEM to mill away the surface of the block between sequential SEM imaging scans of the block's surface, allowing the repeated automated milling/imaging of a sample and building up a 3D dataset for reconstruction^{9,10}. In contrast, serial block face SEM (SBF-SEM) uses an ultramicrotome inside the SEM to remove material from the block face prior to imaging^{11,12}, while array tomography is a nondestructive process that requires the collection of serial sections, onto coverslips, wafers, or tape, prior to setting up an automated workflow of imaging the region of interest in sequential sections in the SEM to generate the 3D dataset¹³. Similar to array tomography, serial section TEM (ssTEM) requires physical sections to be collected ahead of imaging; however, these sections are collected on TEM grids and imaged in a TEM¹⁴⁻¹⁶. ssTEM can be extended by performing tilt tomography¹⁷⁻¹⁹. Serial tilt tomography provides the best resolution in x, y, and z, and while it has been used to reconstruct whole cells²⁰, it is reasonably challenging. This protocol focuses on the practical aspects of ssTEM as the most accessible vEM technique available to many EM labs who may not currently have access to specialized sectioning or vEM instruments but would benefit from generating 3D vEM data.

Serial ultramicrotomy for 3D reconstruction has previously been considered challenging. It was difficult to cut straight ribbons of even section thickness, be able to arrange and pick up ribbons of the correct size, in the correct order, onto grids with sufficient support, but without grid bars obscuring regions of interest, and most importantly, without losing sections, as an incomplete series may prevent full 3D reconstruction²¹. However, improvements to commercial ultramicrotomes, diamond cutting and trimming knives^{22,23}, electron lucent support films on grids^{21,24}, and adhesives for aiding section adhesion and ribbon preservation^{13,21} are just some of the incremental advances over the years that have made the technique more routine in many labs. Once serial sections have been collected, serial imaging in TEM is straightforward and can provide EM images with subnanometer px sizes in x and y, allowing high-resolution interrogation of the subcellular structures—a potential requirement for many research questions. The case study presented here demonstrates the use of ssTEM and 3D reconstruction in the study of endoplasmic reticulum (ER)–organelle contacts in liver hepatocytes. Hepatocytes were the cells where ER–organelle contacts were first observed^{25,26}.

While being contiguous with the nuclear envelope, the ER also makes close contacts with numerous other cell organelles, including lysosomes, mitochondria, lipid droplets, and the plasma membrane²⁷. ER–organelle contacts have been implicated in lipid metabolism²⁸, phosphoinositide and calcium signaling²⁹, autophagy regulation, and stress response^{30,31}. The ER–organelle contacts and other interorganelle contacts are highly dynamic structures that respond to cellular metabolic needs and extracellular cues. They have been shown to vary morphologically in their size and shape and the distances between organelle membranes^{32,33}. It is thought that these ultrastructural differences are likely to reflect their different protein/lipid compositions and function^{34,35}. However, it is still a challenging task to define interorganelle contacts and analyze them³⁶. Hence, a reliable yet simple protocol to examine and characterize interorganelle contacts is required for further investigations.

As ER–organelle contacts can range from 10 to 50 nm in membrane-to-membrane separation, the gold standard for identification has historically been TEM. Thin-section TEM has revealed specific subdomain localization for resident ER proteins at distinct membrane contacts³⁷. Traditionally, this has revealed ER–organelle contacts with nm resolution but often only presented a 2D view of these interactions. However, vEM approaches reveal the ultrastructural presentation and context of these contact sites in 3D, enabling full reconstruction of contacts and more accurate classification of contacts (point vs. tubular vs. cisternal-like) and quantification^{38,39}. In addition to being the first cell type where ER–organelle contacts were observed^{25,26}, hepatocytes have an extensive system of other interorganelle contacts that serve vital roles in their architecture and physiology^{28,40}. However, thorough morphological characterization of ER–organelle and other interorganelle contacts in hepatocytes is still lacking. Accordingly, how interorganelle contacts form and remodel during regeneration and repair is of particular relevance to hepatocyte biology and liver function.

PROTOCOL:

All animals were housed in accordance with the UK Home Office guidelines, and the tissue harvesting was carried out in accordance with the UK Animal (Scientific Procedures) Act 1986.

1. Specimen fixation and preparation

1.1. Dissect the liver tissue into appropriate size pieces, approximately 8 mm x 8 mm x 3 mm, and place the pieces in warm phosphate-buffered saline (PBS, 37 °C).

1.2. Inject room temperature (20–25 °C) fixative (1.5% glutaraldehyde in 1% sucrose, 0.1 M sodium cacodylate) into the liver pieces and transfer them from PBS to fixative for up to 20 min at room temperature. Always keep the tissue submerged in solutions to avoid drying.

NOTE: Aldehydes are irritants that are corrosive and potentially carcinogenic. Sodium cacodylate is toxic if swallowed or inhaled. All fixatives must be handled while wearing appropriate personal protective equipment, and the experiment should be performed in a fume hood. Good fixation will result in a firmer tissue.

1.3. Set up the vibrating microtome with a blade, ice bath, and a cold PBS-filled buffer tray. Mount the first piece of fixed liver tissue on a specimen holder with cyanoacrylate glue and transfer the block to the vibrating microtome.

1.4. Following the manufacturer's recommendations, approach the tissue and slice the fixed liver into 100 µm-thick slices.

1.5. Collect the slices using a spatula or natural hair paintbrush and transfer them into a 12- or 24-well dish containing ice-cold fix (1.5% glutaraldehyde, 0.1 M sodium cacodylate) on ice. Leave the slices on ice until all samples have been sliced and are ready to be processed further.

1.6. Select the slices containing the regions of interest for further processing and wash with gentle agitation. Perform three, 5 min washes with room temperature 0.1 M sodium cacodylate in a 12- or 24-well dish, ensuring the slices have sufficient buffer to move freely.

NOTE: In general, regions of interest are selected based on anatomical features related to the biological question of the study and guided by regions of the tissue that are likely to be present in the entire series, e.g., not on the edge of the section, and that are well preserved.

1.7. In a fume hood, replace 0.1 M sodium cacodylate with freshly prepared 1% osmium tetroxide/1.5% potassium ferricyanide. Place the 12- or 24-well dish in a sealed container and transfer the container to a hazardous-chemicals fridge for 1 h.

NOTE: Osmium is extremely hazardous in case of ingestion, inhalation, and skin contact. Potassium ferricyanide is an irritant and is harmful by inhalation and skin contact. Always handle using appropriate personal protective equipment, and perform the experiment in a fume hood.

1.8. In a fume hood, remove the osmium tetroxide/potassium ferricyanide to a dedicated osmium waste bottle, and wash the samples for 5 min with 0.1 M sodium cacodylate three times. Leave the samples in a sealed container overnight at 4 °C.

NOTE: Potential pause point. Samples can be stored in 0.1 M sodium cacodylate in a sealed container at 4 °C for weeks with little detriment to preservation. Ensure that there is sufficient buffer to prevent drying.

1.9. Incubate the samples with freshly prepared 1% tannic acid in 0.05 M sodium cacodylate for 45 min in the dark at room temperature.

NOTE: Tannic acid is an irritant and can cause eye damage. Wear appropriate personal protective equipment and perform the experiment in a fume hood.

1.10. Perform three 5 min washes with ddH₂O prior to dehydration and embedding.

2. Sample dehydration, Epon resin embedding, and mounting

2.1. Prepare Epon resin according to the following ratio by weight (see step 2.2). Tare a balance with a 100 mL disposable plastic beaker containing a stir bar. Cut the ends from 5 disposable plastic Pasteur pipettes and use these to transfer viscous resin components into the beaker.

2.2. Sequentially add 19.2 g of resin-812, 7.6 g of DDSA, 13.2 g of MNA, and 0.8 g of DMP-30 accelerator into the beaker. Using the fifth clean plastic Pasteur pipette, thoroughly mix the resin components by hand.

NOTE: Avoid introducing bubbles but ensure sufficient mixing of the bottom resin with the top to achieve a color change and rough mixing of the component layers. All resin components are irritants and are harmful by inhalation and skin contact. DMP-30 is corrosive and can cause skin corrosion. Wear appropriate personal protective equipment.

2.3. Place the beaker on a magnetic stirrer and leave to stir gently, periodically giving the resin a manual mix.

2.4. Wash the samples with gentle agitation for 5 min with 70% ethanol; repeat once.

2.5. Wash the samples with gentle agitation for 5 min with 90% ethanol; repeat once.

2.6. Wash the samples with gentle agitation for 5 min with 100% ethanol; repeat once.

2.7. While the samples are in 100% ethanol washes in a fume hood, prepare a 50:50 (v/v) propylene oxide (PO):Epon mixture in a glass vial with a propylene oxide (PO)-resistant plastic lid. Carefully but securely clip on the glass vial lid, and while keeping hold of both lid and vial, shake or vortex to mix.

NOTE: Propylene oxide is an acutely toxic, flammable irritant that dissolves some plastics. Wear appropriate personal protective equipment and perform the experiment in a fume hood.

2.8. After step 2.6, incubate the samples with PO:Epon for 1 h in a PO-resistant container (e.g., aluminum trays or glass vials), with gentle rocking/agitation in the fume hood.

2.9. In the fume hood, transfer the samples to 100% Epon. Incubate for 2 h at room temperature in the fume hood with rocking/rotation/agitation. Transfer the PO:Epon mixture to a dedicated glass Epon waste bottle.

2.10. Repeat step 2.9 once.

2.11. Mount the samples for embedding. Depending on the size of the slices and the region of interest, directly mount the slices onto prepolymerized resin stubs or flat-embed them for dissection and re-embed them at a later date.

NOTE: For flat-embedding, a “cast-a slide” can be used to embed many slices at once. Leftover resin can be used to fill beam capsules and baked to make prepolymerized stubs or frozen for later use.

2.12. Once mounted and covered in sufficient resin to fill the “cast-a slide” cavity, bake the samples overnight in a 60 °C oven.

NOTE: Potential pause point. Samples can be stored at room temperature for years.

2.13. For re-embedding, identify the region of interest in the flat embedded tissue slices. Using a jeweler’s saw, cut out the piece of tissue of appropriate size (1 mm² to 4 mm²) and re-embed using resin prepared, as in step 2.2, onto the top of a prepolymerized block and bake overnight in a 60 °C oven.

NOTE: Alternatively, the tissue piece can be glued to a stub or pin with two-part epoxy resin. Leave to set overnight. Potential pause point.

3. Trimming and serial sectioning of embedded samples

NOTE: Sectioning is a learned skill; users should be proficient at ultrathin sectioning prior to attempting serial sectioning. As exact microtome controls vary across manufacturers, follow the manufacturer’s instructions and guidelines.

3.1. With the sample locked in the trimming adaptor, use a razor blade to carefully trim the resin embedded tissue to meet the following criteria (see **Figure 1A,B**):

3.1.1 Ensure there is a flat, top surface exposing the tissue around the region of interest.

3.1.2 Ensure a trapezoid shape with the top and bottom edges being clean and parallel.

3.1.3 Ensure overall dimensions of 200–500 µm in x, 100–500 µm in y.

3.1.4 Ensure an asymmetric block face, e.g., right-hand side corners of ~90 °, top left corner obtuse, and left-hand bottom corner acute.

NOTE: A trimming cryoknife can be an alternative tool for a razor blade. The other recommendations are for user convenience for ordering sections when imaging. Optional: If sections fail to form stable ribbons, a contact cement can be applied to the leading edge of the block face to aid ribbon formation. Razor blades are sharp; take care to hold the razor blade such that accidental slippages are unlikely to result in personal harm.

[Place Figure 1 here]

3.2. Once trimmed, transfer the specimen arc, together with the chuck and the sample, to the specimen arm of the microtome, positioning the specimen arc so that the arc’s travel range runs from top to bottom; secure the specimen arc in place.

3.3. Place and lock the diamond knife in the knife holder, ensuring that the cutting angle is set appropriately to the knife. Lock the knife holder into the stage securely.

3.4. With the stage uplighting on, use the knife advance while constantly checking the relationship between the block face and the knife's edge. Cautiously advance the knife towards the specimen, continually adjusting the knife's lateral angle, specimen tilt, and specimen rotation by adjusting the relevant knobs until the block is aligned to the knife's edge.

3.5. Turn off the stage uplighting; turn on the stage downlighting; set the top and bottom of the cutting window of the specimen arm; and leave the specimen just below the knife edge.

3.6. Fill the knife boat with clean ddH₂O and ensure the water surface is level with the knife's edge and just slightly concave.

3.7. Optional: Dip an eyelash into the 0.1% Triton X-100 and then in the knife boat water to reduce the surface tension of the water to aid chloroforming and ribbon pickup.

3.8. Prepare the workstation with eyelashes (eyelash glued to a cocktail stick), formvar-coated slot grids, labeled crossover forceps, chloroform, 0.1% Triton X-100 solution, distilled water, filter paper, and grid box with grid box notes.

3.9. Set the cutting speed at 1 mm/s and the initial cutting thickness to 100 nm and start the cutting cycle.

3.10. After the first section is cut, change the cutting parameters to a cutting speed at 0.8 mm/s and the cutting thickness to 70 nm, and continue cutting, allowing sections to form a ribbon moving down the surface of the water-filled knife boat (**Figure 1C**).

NOTE: It is important to be aware of the color of the sections being produced as this is often a more accurate guide to the thickness of the resin sections. Silver sections are usually around 70 nm thick, while grey sections are thinner and gold sections are thicker.

3.11. Allow the microtome to continue cutting sections and the ribbon to get longer.

NOTE: It is important to avoid large vibrations and physical disturbances in the room. Drafts can cause the sections to move on the surface of the water in the knife boat, and physical vibrations can cause the microtome to cut unevenly.

3.12. Once enough sections are collected and before the ribbon gets to the end of the boat, stop the cutting (just after the sample has passed the knife's edge).

NOTE: The number of sections needed depends on the size of the block face and the size of the dataset to be collected. Thus, it is useful to be aware of the relationship between the size of the block and the slot grid as the cut sections are coming off.

3.13. Using an eyelash in each hand, gently break the ribbon into smaller ribbons that can fit in the length of the slot grid, taking care to make a note of their relative positions from within the sample.

NOTE: If their combined width fits, multiple ribbons can be gently placed next to each other and picked up together in a single slot grid. If picking up multiple ribbons on a single slot grid, pay attention to the order and the relative position of the ribbons. For example, always place the ribbons further into the sample to the right of a ribbon already in the sample (**Figure 1D**).

3.14. Optional: Using a glass applicator rod, hover a drop of chloroform over the sections to flatten them out.

NOTE: Chloroform is toxic and an irritant. Do not let chloroform touch the water surface or sections. If it accidentally does, the water needs to be removed and the knife washed before returning to sectioning. The chloroform can damage the sections and degrade the glue that secures the diamond into the knife boat.

3.15. Using the first numbered forceps, pick up the first empty slot grid (on the right-hand side of the slot, formvar side down), gently dip in the Triton X-100, and then twice in the distilled water before removing excess water from the forceps edge using a piece of filter paper.

3.16. With an eyelash in one hand and the forceps in the other hand, gently lower approximately 2/3rd of the formvar-coated slot grid into the water of the knife boat (away from the sections), so that the formvar side is facing down, and the right-hand long edge of the slot is at the surface of the water and parallel to the water's edge.

3.17. Gently waft the grid in the water towards the ribbons so that upon the return stroke, the sections drift towards the grid. Continue to do this in smaller and smaller wafts until the right-hand edge of the ribbon lines up with the right-hand edge of the slot. Then, with the last waft, gently bring the grid up to pick the sections up into the slot grid.

3.18. Leave the grid in the forceps to dry before storing it in the grid box, appropriately annotated on the grid box reference sheet.

3.19. Repeat step 3.16 until all ribbons are collected, ensuring that the order of ribbons is maintained.

3.20. If further sections are required, retract the knife 150 nm or so, check the water level in the boat, and add more if required. Start the cutting process again, following steps 3.11–3.18.

3.21. Once all sections are collected, ensure the knife edge is free from section debris, retract the knife away from the block face, and remove and clean the knife.

4. Grid staining

4.1. Once dry, stain the sections with Reynolds' lead citrate either on parafilm on the bench or in a Petri dish. Place several pellets of sodium hydroxide under a Petri dish lid to provide a carbon dioxide-free environment. Then, carefully, away from the pellets, pipette 40 μ L drops of Reynolds' lead citrate on the parafilm, one for each grid.

NOTE: Do not stain too many grids at once; e.g., the maximum should be 6. Try not to breathe directly on the staining dish. Carbon dioxide can react with the lead citrate and cause unwanted precipitate on the grids.

4.2. Invert each grid (section side down) onto the lead citrate drop and leave protected by the Petri dish lid for 7 to 10 min. While the grids are staining, prepare a larger second piece of parafilm on the bench with five 300 μ L drops of distilled water for each grid.

4.3. At the end of the lead citrate incubation, transfer each grid to a droplet of distilled water to wash for 1 min without breathing directly on the grids.

4.4. Repeat step 4.3 a total of five times.

4.5. Using numbered crossover forceps, pick up the first grid, touch the edge of the grid to filter paper to wick away most of the water, and allow to dry in the forceps (for at least 20 min). Repeat for each grid.

5. Imaging acquisition by TEM

NOTE: As exact TEM controls vary across manufacturers, follow the manufacturer's instructions and guidelines. The following steps should be performed by users who are already proficient at TEM use.

5.1. Prior to imaging, perform the usual checks, e.g., beam alignment, gain references, and sample eucentricity.

5.2. Carefully load the first grid of serial sections into the specimen holder, taking care to align the slot (and therefore sections) to the vertical axis of the microscope stage.

NOTE: This accuracy is not essential but saves time during acquisition and future data handling stages. When inserting the grid (section side down or section side up), take care to image all grids in the same orientation.

5.3. At low magnification, observe the order, location, and position of the serial sections (Figure 1E). Navigate to the middle section of the series on the grid.

NOTE: Depending on the exact research aim, approaches for imaging may vary; however, the following is a useful starting point. The shape of the sections and the relationship of the ribbons (as picked up in step 3.14) dictate which section was first and which section was last on the grid.

5.4. Browse the sample and identify a region of interest. Observe the sample at the desired magnification, and consider collecting the series at a slightly lower magnification, as sections are often not perfectly aligned, and images may need to be cropped later.

5.5. Take reference images at lower magnifications to appreciate the context of the region of interest, its rough location at different magnifications in relation to section boundaries, and landmark features within the sample. Use these to sign-post the region of interest in other sections.

5.6. Optional: for screen referencing, use reusable adhesive putty, stickers, or a piece of overhead projector (OHP) paper, taped to the screen, to place temporary markers on the screen to allow routine reimaging of the same features of the region of interest in the center of the image, throughout the dataset (see yellow stars in **Figure 1E**).

5.7. Using the reference images, navigate to the region of interest on the first section of the grid, and acquire an image at the desired magnification.

NOTE: When saving images, note down the first file name of the first image of the series, and use sequential naming nomenclature so that all image names follow the sequential order of the serial sections.

5.8. Navigate to the next section and repeat step 5.7 until all sections have been imaged for that region of interest.

6. Image export and serial section alignment registration

6.1. Export the image files belonging to the same stack into a single folder. Make sure the folder is sorted by file name.

NOTE: The images should ideally have the same root name and follow the order in which they have been acquired.

6.2. Open Fiji and click on **File | Import | Image Sequence**.

6.3. Click on the first image of the folder and click **Open**. Wait for a popup window of **Sequence Options** to appear (**Figure 2A**).

[Place Figure 2 here]

6.4. Click **Sort names numerically | Convert to 8-bit** option. Press **OK**.

NOTE: Conversion to 8-bit aids import of the data into Amira and reduces the file size, allowing quicker processing speeds in later steps.

6.5. Check the completeness, sequence, and magnification of the created stack. Save the created stack as a .tif file.

NOTE: Images should have been acquired at the same magnification.

6.6. Execute the TrakEM2 plugin⁴¹. Go to **File | New | TrackEM2 (blank)**.

NOTE: The plugin will ask the user to save the TrackEM2 files. If needed, save the TrackEM2 files to the image folder. Three windows should appear: a project window, a stack navigation (left) window, and a stack visualization pane (**Figure 2B**).

6.7. Right-click to the black visualization pane. Click **Import | Import stack** and select the previously created stack.

6.8. Click **OK** to load the stack to the stack navigation window.

NOTE: A Slice separation window will pop up to ask for pixel and dimension relationship. For only stack alignment, click **OK** to skip this step.

6.9. Use the slider to check all the slices of the stack. Look for the loaded slice, which will appear as a patch in the navigation plan. Select the patches that will be included in the following alignment.

NOTE: Selected patches will go blue.

6.10. Hover the mouse over the viewing pane. Right-click the image, select **Align | Align stack slices (Figure 2C-1)**.

6.11. Specify the alignment parameters through a set of three sequential windows.

NOTE: For most data, start with a rigid alignment (allows for rotation and translation but not transformation) and keep other parameters as default (**Figure 2C-2**).

6.12. Allow the alignment to run until the readout log says **Montage done**.

NOTE: Runtime depends on the number of voxels and the speed of the computer.

6.13. Check the aligned stack in the viewing pane. Press **Alt** and - keys (in PC) or the **Ctrl** and - keys (in Mac) for a zoom-out view of the aligned stack.

6.14. If satisfied with the aligned stack, right-click **Export | Make flat image** to save the aligned stack.

6.15. Select the first image as the start of the stack and the last image as the end of the stack, click **OK (Figure 2C-3)**. Save the aligned stack as .tif.

NOTE: To reduce file size, crop the data to only contain the necessary region of interest.

6.16. If needed, execute an affine alignment on the aligned stack. Open the aligned stack in Fiji, select **Plugin | Registration | StackReg**.

6.17. Choose the **affine** option and press **OK**. Wait until the program is complete.

6.18. Save the affine-aligned stack with a different file name.

7. Segmentation and 3D reconstruction

7.1. Open Amira⁴². Click **File | Open Data** to load the aligned stack.

7.2. Specify the voxel measurements in the new popup window (**Figure 3A**).

[Place Figure 3 here]

NOTE: An image stack node will appear in the project interface, and an orthoslice will appear in the viewing pane on the right (**Figure 3B**).

7.3. To start segmentation, select the **Segmentation Tab** (**Figure 3B**).

NOTE: It is recommended to save the segmentation progress before and during the segmentation. Go to **Model | Save Model As** any .am file that suits.

7.4. Click **New** in the segmentation editor panel to define new objects in the material list. Right-click to change the color of the object and double-click to rename the object.

7.5. For manual segmentation, choose the **segmentation** tool below the material list. Select the default **Brush** tool to highlight the pixels (**Figure 3C**).

NOTE: Alternatively, use the **brush** tool to trace the outline of the object and press **Shift + F** to fill the object.

7.6. To convert the **brush** tool into an **eraser**, continually press **Ctrl** while selecting pixels for correction. Annotate every slice in the stack.

7.7. Once confirmed, assign the selection to a label by clicking the **+** sign. Click the **-** sign to remove the selection.

7.8. Go back to the project interface once the segmentation is complete. Look for a node with a ".label" extension connected to the image stack.

7.9. Right-click the ".label" extension and select **Generate Surface | Apply** to create a .surf file.

7.10. To render the 3D model of a segmented object, right-click the .surf file and select **Surface view** to generate a 3D model in the viewing pane.

7.11. Save the 3D model for visualization or further quantitative analyses.

REPRESENTATIVE RESULTS:

For this technique, regions of interest are selected based on the biological research aim and identified prior to the trimming and sectioning of embedded tissue. Similarly, the size of the block face may be dictated by the research question; in this case, the sample was trimmed to leave a block face of approximately 0.3 mm x 0.15 mm (**Figure 4A**). This allowed for two grids of 9 serial sections per grid, providing 18 serial sections and incorporating a volume of liver tissue of a volume of approximately $62 \mu\text{m}^3$ ($316 \mu\text{m} \times 150 \mu\text{m} \times 1.3 \mu\text{m}$). This volume was sufficient to allow the complete 3D reconstruction of individual mitochondria in liver tissue.

[Place Figure 4 here]

Visualization of the serial sections by TEM at low magnification helps to identify the designated area of interest and its context within the rest of the tissue (**Figure 4B**). These images can be used to find the same region of interest in subsequent sections. A region of interest showing good preservation at a boundary between two apposed hepatocytes was selected and presented here. Higher magnification imaging allows the observation of the morphological details of the different organelles (**Figure 4C**) with nm resolution. To illustrate two types of ER–organelle associations, selected mitochondria and the ER were segmented, manually tracing the edge of the membranes presenting with enhanced electron density. Afterward, the brush tool was set to a fixed nm/px thickness (**Figure 3B**) and used to follow the boundary of the organelle of interest to highlight the regions between the two targeted organelles that were within a specified contact distance to one another and could be designated as a particular class of organelle contacts. **Figure 4D** shows a tilted orthoslice overlaid with segmentation traces and its relative position (arrowhead in the inlet 3D model) within the whole mitochondrion.

The traces were assigned different colors, reconstructed into a 3D model after segmentation, and displayed at different orientations (**Figure 4E**). The ER (yellow) structure was shown to be partially transparent in the middle panels to visualize the ER–mitochondria contacts and mitochondria (cyan) underneath. The front and rear views of the model reveal an asymmetrical distribution of interorganelle contacts of different intermembrane spacings. Intermembrane space smaller than 21 nm was assigned as ER–mitochondria contact (pink) because functions such as lipid transfer have been reported to be feasible at this distance⁴³. The intermembrane space (blue) between 21 and 100 nm was also annotated because this region may represent the recently reported mitochondria–rough-ER associations⁴⁴. Wrapping ER structures of similar curvature were observed in the 3D model (**Figure 4E**). **Figure 4D** shows an example of changing intermembrane distance ($\sim 40 \text{ nm} \rightarrow \sim 20 \text{ nm} \rightarrow \sim 40 \text{ nm}$) between the wrapping ER cisternae and the mitochondria. The method allows follow-up patch analysis of these two distinct intermembrane spaces, such that quantitative analysis of their abundance, distribution, and topology is possible.

FIGURE AND TABLE LEGENDS:

Figure 1: Serial section TEM workflow. (A) Diagram of the specimen in the resin block. (B) Trim block to generate a trapezoid shape with edges suitable for serial sectioning and asymmetric block face to ensure known orientation. (C) Diagram showing ribbons of serial sections, floating on the water's surface in the diamond knife boat. (D) Diagram showing the section and ribbon organization, dictating order of sections, on a 3 mm diameter TEM slot

grid. (E) TEM imaging and navigation. Showing ribbon and section order and using “yellow star stickers” on the monitor for screen referencing to ensure reimaging of the same region of interest in subsequent sections. (F) Image alignment and cropping. (G) Segmentation, 3D reconstruction, and visualization. Abbreviation: TEM = transmission electron microscopy.

Figure 2: Creation of a serial stack and serial section alignment using Fiji. (A) Screenshot showing the Sequence Options when loading the images for making a serial stack. (B) Screenshot of the TrackEM2 plugin and the key windows of the plugin. Press **OK** in the Slice separation to proceed with the alignment. (C) Screenshot after successfully loading the serial stack into the visualization pane. Three sequential windows of alignment parameters will pop up once **Align stack slices** are selected. Export the aligned stack once the alignment is completed.

Figure 3: Segmentation of serial stack using Amira. (A) The Voxel definition popup window prior to loading an aligned stack. (B) Screenshot of the project interface after the import of a stack. Select the **Segmentation tab** to start object tracing in the **Segmentation Editor** panel. (C) Key features of the segmentation tab. Define the objects for segmentation in the **Segmentation Editor** section of the **Segmentation tab**. Use the **zoom** function to assist identification of objects. Select the **Brush** tool and trace the boundary of the object. Click the **+** symbol under **Selection** to assign the trace. An assigned object will appear to have a red boundary in the orthoslice viewing pane.

Figure 4: Segmentation and 3D reconstruction reviewing the morphology of ER and associated ER–mitochondria contacts. (A) Overview of ribbon of serial sections in the TEM. (B) Low-magnification view of region of interest and contextual landmarks for relocation. Scale bars = 40 μm (i), 20 μm (ii), 5 μm (iii), 1 μm (iv). (C) Left: EM tomogram of two apposed hepatocytes. Right: segmented version of the same tomogram. Trace of the ER (yellow), mitochondria (cyan), and intermembrane contacts between the ER and mitochondria of different space: 0–20 nm (magenta); 21–100 nm (blue). (D) An orthoslice isolated from the reconstructed model showing only the ER and the different membrane contacts, corresponding to the arrow annotated region in the inset. (E) 3D reconstruction of the segmented organelles and ER–mitochondria contacts at different angles. Abbreviations: ER = endoplasmic reticulum; TEM = transmission electron microscopy; mt = mitochondria.

Table 1: Overview of volume electron microscopy techniques. Abbreviations: EM = electron microscopy; TEM = transmission EM; FIB-SEM = focused ion beam SEM; SBF-SEM = serial block face SEM; SEM + AT = SEM with Array Tomography.

DISCUSSION:

An accessible vEM technique for visualizing organelle structure and interactions in 3D is described in this protocol. The morphology of interorganelle contacts in hepatocytes is presented as a case study here. However, this approach has also been applied to investigate a variety of other samples and research areas, including Schwann cell–endothelial interactions in peripheral nerves⁴⁵, Weibel Palade Body biogenesis in endothelial cells⁴⁶, cargo secretion in kidney cells⁴⁷, and synapse morphology in hippocampal neurons⁴⁸. To better understand liver biology, this approach can be used to investigate hepatocyte morphology in 2D cell culture, 3D hepatic organoid model systems⁴⁹, and liver tissue. This robust and flexible

approach can be used by many laboratories with access to a conventional 120 kV transmission electron microscope and ultramicrotome and does not require expensive sample preparation techniques.

While this is an accessible protocol, it is important to note that there are alternative vEM techniques that can provide certain advantages to the researcher, depending on the research question; see **Table 1** for an overview^{6,50,51}. Often the resolution and volume of the data needed directly influence the researchers' choice of the vEM technique and the ease and speed at which the project can progress. FIB-SEM, for example, can remove very thin layers from the sample prior to imaging, resulting in excellent z-resolution (z thickness as low as 4 nm) and potentially providing volumetric 3D data with isotropic voxels. This allows visualization of the data with equal resolution from every angle, which can sometimes provide distinct advantages when contact points are difficult to discern^{52,53}. FIB-SEM can generate large volumes but is often costly and time-consuming, while SBF-SEM is an excellent technique to use when larger volumes are required, e.g., 100s to 1000s of sections⁵⁴. SBF-SEM and array tomography provide similar xy resolution as FIB-SEM but with reduced z-resolution. As array tomography involves collecting physical sections, the z-resolution is perhaps the poorest of its competitors (z thickness 50+ nm) but has several distinct advantages. Foremost, because it is a nondestructive technique, the sample can be revisited at different xy resolutions, with easy montaging, at various times, and across numerous regions, allowing full context and detail to be appreciated in a single sample. Serial section TEM also shares this benefit; however, as sections need to be collected onto TEM grids, it is better suited to smaller volumes that require fewer sections to be collected prior to imaging. However, it is compatible with TEM tilt tomography, a technique that provides very high z-resolution (z thickness as low as 2 nm) of very small volumes, enabling further interrogation of specific contact sites of interest if required.

Regardless of the vEM approach taken, sample preservation is critical to the success of the project. The fixation medium should be an isotonic match to the tissues, and the transfer to the fixation medium should be done rapidly to avoid drying of the tissues⁵⁵. Liver tissue can be challenging to preserve, and while it offers excellent preservation, allowing retention of liver tissue for additional experiments, whole liver perfusion for electron microscopy is often not possible. Liver-wedge needle perfusion is an excellent alternative⁵⁶. Cryoimmobilization is also an option but requires immediate high-pressure freezing to achieve homogeneous vitrification of fresh vibratome sections; thus, this approach is quite challenging. After initial fixation, there are a variety of EM specimen preparation protocols that yield satisfactory results. A routine TEM protocol is presented here⁵⁷, but "enbloc megametal" protocols have also been successfully employed with other biological samples^{45,58}. While these "enbloc megametal" protocols provide more contrast in the sample, giving some structures a more heavily stained appearance, they also have the advantage of removing the requirement to stain sections, thus reducing the risk of adding unwanted stain precipitate on samples and damaging grids in the process.

Another critical step in this protocol is ultrathin sectioning and ribbon collection. Collecting serial sections from the water surface of the cutting boat is a manual process that could lead to damaged and missing sections. For example, should sections fail to adhere to each other and form stable ribbons, contact cement can be applied to the leading edge of the blockface

to stabilize the ribbons¹³. The duration and routine success of this step are skill-dependent⁵⁹. Although a plethora of model-specific section-picking methods^{60,61} may confuse beginners, some simple, practical guides^{55,62} for routine sectioning, together with practice, can significantly improve sectioning skills. This protocol requires minimal specialist equipment, and with the aid of video footage showing the practical aspects of manual manipulation techniques during sectioning, ribbon detachment, and ribbon handling and pickup, provides an excellent beginner's guide to serial sectioning.

Volume EM image analysis continues to be an area of development with a variety of open-source and commercial software options currently available, and the list is ever-growing. A selection of software for alignment (TrakEM2⁴¹), 3D segmentation, and reconstruction (Amira⁴²) are presented here; however, many alternatives are available for alignment (e.g., Fiji, Register Virtual Slices⁶³, Atlas5, and 3D reconstruction (e.g., MIB⁶⁴; Reconstruct⁶⁵; IMOD⁶⁶). For relatively small analysis projects, regardless of whether the data are generated locally or sourced from openly shared datastores (EMPIAR⁶⁷, Open Organelle⁶⁸), manual segmentation described here is an accessible and feasible option. However, for larger datasets, many users are turning to machine learning and artificial intelligence for automation of these tasks^{69,70}, as well as crowd-sourcing volunteers⁷¹ or combining both⁷².

Ultimately, after alignment and 3D segmentation, 3D reconstruction reveals not only the morphology of the structures in question but, importantly, also their relationship with other organelles, including the unique characteristics of any contact sites present. These organelle contacts can be analyzed further, and features such as the number of contacts, contact area, volumes of organelles, and morphometric parameters of the organelles can be extracted and compared between experimental models⁷⁰. Quantitation options are numerous, and their relevance varies hugely depending upon the exact research question. Hence, they have not been covered in depth as part of this protocol.

Pathological processes affecting organelle contacts have been implicated in both the rare (e.g., Wilson's disease) and common (viral hepatitis and nonalcoholic steatohepatitis) disorders⁷³⁻⁷⁵. For example, the ER-mitochondria and mitochondria-lipid droplet contact sites appear to regulate lipid metabolism in hepatocytes; therefore, the study of these contacts is of great interest. In conclusion, serial section TEM and subsequent 3D reconstruction and analysis is a powerful technique to interrogate interorganelle contacts and probe their relative importance in liver functions and diseases.

ACKNOWLEDGMENTS:

We thank Joanna Hanley, Rebecca Fiadeiro, and Ania Straatman-Iwanowska for expert technical assistance. We also thank Stefan lab members and Ian J. White for helpful discussions. J.J.B. is supported by MRC funding to the MRC Laboratory of Molecular Cell Biology at UCL, award code MC_U12266B. C.J.S. is supported by MRC funding to the MRC Laboratory of Molecular Cell Biology University Unit at UCL, award code MC_UU_00012/6. P.G. is funded by the European Research Council, grant code ERC-2013-StG-337057.

DISCLOSURES:

The authors have no conflicts of interest to disclose.

REFERENCES:

- 1 Knoll, M., Ruska, E. Das elektronenmikroskop. *Zeitschrift für Physik*. **78** (5), 318–339 (1932).
- 2 von Ardenne, M. Das elektronen-rastermikroskop. *Zeitschrift für Physik*. **109** (9), 553–572 (1938).
- 3 Bang, B. H., Bang, F. B. Graphic reconstruction of the third dimension from serial electron microphotographs. *Journal of Ultrastructure Research*. **1** (2), 138–139 (1957).
- 4 Birch-Andersen, A. Reconstruction of the nuclear sites of Salmonella typhimurium from electron micrographs of serial sections. *Journal of General Microbiology*. **13** (2), 327–329 (1955).
- 5 Denk, W., Horstmann, H. Serial block-face scanning electron microscopy to reconstruct three-dimensional tissue nanostructure. *PLoS Biology*. **2** (11), e329 (2004).
- 6 Peddie, C. J., Collinson, L. M. Exploring the third dimension: volume electron microscopy comes of age. *Micron*. **61**, 9–19 (2014).
- 7 Titze, B., Genoud, C. Volume scanning electron microscopy for imaging biological ultrastructure. *Biology of the Cell*. **108** (11), 307–323 (2016).
- 8 Kornfeld, J., Denk, W. Progress and remaining challenges in high-throughput volume electron microscopy. *Current Opinion in Neurobiology*. **50**, 261–267 (2018).
- 9 Heymann, J. A. et al. Site-specific 3D imaging of cells and tissues with a dual beam microscope. *Journal of Structural Biology*. **155** (1), 63–73 (2006).
- 10 Knott, G., Marchman, H., Wall, D., Lich, B. Serial section scanning electron microscopy of adult brain tissue using focused ion beam milling. *Journal of Neuroscience*. **28** (12), 2959–2964 (2008).
- 11 Leighton, S. B. SEM images of block faces, cut by a miniature microtome within the SEM - a technical note. *Scanning Electron Microscopy*. (Pt 2), 73–76 (1981).
- 12 Martone, M. E., Deerinck, T. J., Yamada, N., Bushong, E., Ellisman, M. H. Correlated 3D light and electron microscopy: use of high voltage electron microscopy and electron tomography for imaging large biological structures. *Journal of Histotechnology*. **23** (3), 261–270 (2000).
- 13 Micheva, K. D., Smith, S. J. Array tomography: a new tool for imaging the molecular architecture and ultrastructure of neural circuits. *Neuron*. **55** (1), 25–36 (2007).
- 14 Sjostrand, F. S. Ultrastructure of retinal rod synapses of the guinea pig eye as revealed by three-dimensional reconstructions from serial sections. *Journal of Ultrastructure Research*. **2** (1), 122–170 (1958).
- 15 Ware, R. W. Three-dimensional reconstruction from serial sections. *International Review of Cytology*. **40**, 325–440 (1975).
- 16 Stevens, J. K., Davis, T. L., Friedman, N., Sterling, P. A systematic approach to reconstructing microcircuitry by electron microscopy of serial sections. *Cognitive Brain Research*. **2** (3), 265–293 (1980).
- 17 Hoppe, W. Three-dimensional electron microscopy. *Annual Review of Biophysics*. **10**, 563–592 (1981).
- 18 Frank, J. *Electron tomography: methods for three-dimensional visualization of structures in the cell*. Springer, New York, NY (2008).
- 19 Baumeister, W. Electron tomography: towards visualizing the molecular organization of the cytoplasm. *Current Opinion in Structural Biology*. **12** (5), 679–684 (2002).

793 20 Hoog, J. L., Schwartz, C., Noon, A. T., O'Toole, E. T. Organization of interphase
794 microtubules in fission yeast analyzed by electron tomography. *Developmental Cell*. **12** (3),
795 349–361 (2007).

796 21 Harris, K. M., Perry, E., Bourne, J., Feinberg, M., Ostroff, L., Hurlburt, J. Uniform serial
797 sectioning for transmission electron microscopy. *Journal of Neuroscience*. **26** (47), 12101–
798 12103. (2006).

799 22 Jesior, J. C. Use of low-angle diamond knives leads to improved ultrastructural
800 preservation of ultrathin sections. *Scanning Microscopy Supplement*. **3**, 147–152; discussion
801 152–143 (1989).

802 23 Studer, D., Gnaegi, H. Minimal compression of ultrathin sections with use of an
803 oscillating diamond knife. *Journal of Microscopy*. **197** (Pt 1), 94–100 (2000).

804 24 Gay, H., Anderson, T. F. Serial sections for electron microscopy. *Science*. **120** (3130),
805 1071–1073 (1954).

806 25 Bernhard, W., Rouiller, C. Close topographical relationship between mitochondria
807 and ergastoplasm of liver cells in a definite phase of cellular activity. *The Journal of*
808 *Biophysical and Biochemical Cytology*. **2** (4 Suppl), 73–78 (1956).

809 26 Palade, G. E. An electron microscope study of the mitochondrial structure. *The*
810 *Journal of Histochemistry & Cytochemistry*. **1** (4), 188–211 (1953).

811 27 Wu, H., Carvalho, P., Voeltz, G. K. Here, there, and everywhere: The importance of
812 ER membrane contact sites. *Science*. **361** (6401), eaan5835 (2018).

813 28 Vance, J. E. Inter-organelle membrane contact sites: implications for lipid
814 metabolism. *Biology Direct*. **15** (1), 24 (2020).

815 29 Stefan, C. J. Endoplasmic reticulum-plasma membrane contacts: Principals of
816 phosphoinositide and calcium signaling. *Current Opinion in Cell Biology*. **63**, 125–134 (2020).

817 30 Zaman, M. F., Nenadic, A., Radojicic, A., Rosado, A., Beh, C. T. Sticking with it: ER-PM
818 membrane contact sites as a coordinating nexus for regulating lipids and proteins at the cell
819 cortex. *Frontiers in Cell and Developmental Biology*. **8**, 675 (2020).

820 31 van Vliet, A. R., Sassano, M. L., Agostinis, P. The unfolded protein response and
821 membrane contact sites: tethering as a matter of life and death? *Contact*. **1**, 1–15 (2018).

822 32 Cohen, S., Valm, A. M., Lippincott-Schwartz, J. Interacting organelles. *Current Opinion*
823 *in Cell Biology*. **53**, 84–91 (2018).

824 33 Hariri, H. et al. Lipid droplet biogenesis is spatially coordinated at ER-vacuole
825 contacts under nutritional stress. *EMBO Reports*. **19** (1), 57–72 (2018).

826 34 Stefan, C. J., Trimble, W. S., Grinstein, S., Drin, G. Membrane dynamics and organelle
827 biogenesis-lipid pipelines and vesicular carriers. *BMC Biology*. **15** (1), 102 (2017).

828 35 Eisenberg-Bord, M., Shai, N., Schuldiner, M., Bohnert, M. A tether is a tether is a
829 tether: tethering at membrane contact sites. *Developmental Cell*. **39** (4), 395–409 (2016).

830 36 Scorrano, L., De Matteis, M. A., Emr, S., Giordano, F. Coming together to define
831 membrane contact sites. *Nature Communications*. **10** (1), 1287 (2019).

832 37 Lak, B., Li, S., Belevich, I., Sree, S. Specific subdomain localization of ER resident
833 proteins and membrane contact sites resolved by electron microscopy. *European Journal of*
834 *Cell Biology*. **100** (7), 151180 (2021).

835 38 Collado, J., Kalemanov, M., Campelo, F., Bourgoint, C. Tricalbin-mediated contact
836 sites control ER curvature to maintain plasma membrane integrity. *Developmental Cell*. **51**
837 (4), 476–487 e477 (2019).

- 39 West, M., Zurek, N., Hoenger, A., Voeltz, G. K. A 3D analysis of yeast ER structure reveals how ER domains are organized by membrane curvature. *Journal of Cell Biology*. **193** (2), 333–346 (2011).
- 40 Ilacqua, N., Anastasia, I., Raimondi, A., Lemieux, P. A three-organelle complex made by wrapper contacts with peroxisomes and mitochondria responds to liver lipid flux changes. *Journal of Cell Science*. **135** (5), jcs259091 (2022).
- 41 Cardona, A., Saalfeld, S., Schindelin, J., Arganda-Carreras, I. TrakEM2 software for neural circuit reconstruction. *PLoS One*. **7** (6), e38011 (2012).
- 42 Stalling, D., Westerhoff, M., Hege, H.-C. Amira: A highly interactive system for visual data analysis. *The Visualization Handbook*. **38**, 749–767 (2005).
- 43 Hsieh, T. S., Chen, Y. J., Chang, C. L., Lee, W. R., Liou, J. Cortical actin contributes to spatial organization of ER-PM junctions. *Molecular Biology of the Cell*. **28** (23), 3171–3180 (2017).
- 44 Anastasia, I., Ilacqua, N., Raimondi, A., Lemieux, P. Mitochondria-rough-ER contacts in the liver regulate systemic lipid homeostasis. *Cell Reports*. **34** (11), 108873 (2021).
- 45 Cattin, A. L., Burden, J. J., Van Emmenis, L., Mackenzie, F. E. Macrophage-Induced Blood Vessels Guide Schwann Cell-Mediated Regeneration of Peripheral Nerves. *Cell*. **162** (5), 1127–1139 (2015).
- 46 Lopes-da-Silva, M. et al. A GBF1-dependent mechanism for environmentally responsive regulation of ER-Golgi transport. *Developmental Cell*. **49** (5), 786–801 e786 (2019).
- 47 Banushi, B., Forneris, F., Straatman-Iwanowska, A., Strange, A. Regulation of post-Golgi LH3 trafficking is essential for collagen homeostasis. *Nature Communications*. **7**, 12111 (2016).
- 48 Rey, S. A. et al. Ultrastructural and functional fate of recycled vesicles in hippocampal synapses. *Nature Communications*. **6**, 8043 (2015).
- 49 Belicova, L., Repnik, U., Delpierre, J., Gralinska, E. Anisotropic expansion of hepatocyte lumina enforced by apical bulkheads. *Journal of Cell Biology*. **220** (10), e202103003 (2021).
- 50 Kizilyaprak, C., Daraspe, J., Humbel, B. M. Focused ion beam scanning electron microscopy in biology. *Journal of Microscopy*. **254** (3), 109–114 (2014).
- 51 Xu, C. S., Hayworth, K. J., Lu, Z., Grob, P. Enhanced FIB-SEM systems for large-volume 3D imaging. *Elife*. **6**, 1–36 (2017).
- 52 Parlakgöl, G., Arruda, A.P., Cagampan, E., Pang, S. High resolution 3D imaging of liver reveals a central role for subcellular architectural organization in metabolism. *bioRxiv*. <https://www.biorxiv.org/content/biorxiv/early/2020/11/18/2020.11.18.387803.full.pdf> (2020).
- 53 Guerin, C. J., Kremer, A., Borghgraef, P., Lippens, S. Targeted studies using serial block face and focused ion beam scan electron microscopy. *The Journal of Visualized Experiments: JoVE*. (150), doi. 10.3791/59480 (2019).
- 54 Kremer, A. et al. A workflow for 3D-CLEM investigating liver tissue. *Journal of Microscopy*. **281** (3), 231–242 (2021).
- 55 Hayat, M. *Principles and techniques of electron microscopy: biological applications*. Cambridge University Press (2000).
- 56 Wisse, E., Braet, F., Duimel, H., Vreuls, C. Fixation methods for electron microscopy of human and other liver. *World Journal of Gastroenterology*. **16** (23), 2851–2866 (2010).

884 57 Hanley, J., Dhar, D. K., Mazzacuva, F., Fiadeiro, R. Vps33b is crucial for structural and
885 functional hepatocyte polarity. *Journal of Hepatology*. **66** (5), 1001–1011 (2017).

886 58 Deerinck, T. J., Bushong, E. A., Thor, A., Ellisman, M. H. NCMIR methods for 3D EM: a
887 new protocol for preparation of biological specimens for serial block face scanning electron
888 microscopy. *Microscopy*. **1**, 6–8 (2010).

889 59 Miranda, K., Girard-Dias, W., Attias, M., de Souza, W., Ramos, I. Three dimensional
890 reconstruction by electron microscopy in the life sciences: An introduction for cell and tissue
891 biologists. *Molecular Reproduction and Development*. **82** (7–8), 530–547 (2015).

892 60 Yamaguchi, M., Chibana, H. A method for obtaining serial ultrathin sections of
893 microorganisms in transmission electron microscopy. *The Journal of Visualized Experiments:*
894 *JoVE*. (131), 56235 (2018).

895 61 Hall, D. H., Hartwig, E., Nguyen, K. C. Modern electron microscopy methods for *C.*
896 *elegans*. *Methods in Cell Biology*. **107**, 93–149 (2012).

897 62 Hagler, H. K. Ultramicrotomy for biological electron microscopy. *Methods in*
898 *Molecular Biology*. **369**, 67–96 (2007).

899 63 Arganda-Carreras, I. et al. Consistent and elastic registration of histological sections
900 using vector-spline regularization. In *Computer vision approaches to medical image analysis*.
901 Beichel, R. R., Sonka, M. (Eds), CVAMIA 2006, Lecture Notes in Computer Science, Springer
902 Berlin Heidelberg, Berlin, Heidelberg, **4241**, 85–95 (2006).

903 64 Belevich, I., Joensuu, M., Kumar, D., Vihinen, H., Jokitalo, E. Microscopy image
904 browser: a platform for segmentation and analysis of multidimensional datasets. *PLoS*
905 *Biology*. **14** (1), e1002340 (2016).

906 65 Fiala, J. C. Reconstruct: a free editor for serial section microscopy. *Journal of*
907 *Microscopy*. **218** (Pt 1), 52–61 (2005).

908 66 Kremer, J. R., Mastronarde, D. N., McIntosh, J. R. Computer visualization of three-
909 dimensional image data using IMOD. *Journal of Structural Biology*. **116** (1), 71–76 (1996).

910 67 Iudin, A., Korir, P. K., Salavert-Torres, J., Kleywegt, G. J., Patwardhan, A. EMPIAR: a
911 public archive for raw electron microscopy image data. *Nature Methods*. **13** (5), 387–388
912 (2016).

913 68 Xu, C. S., Pang, S., Shtengel, G., Muller, A. An open-access volume electron
914 microscopy atlas of whole cells and tissues. *Nature*. **599** (7883), 147–151 (2021).

915 69 Karabag, C. et al. Semantic segmentation of HeLa cells: An objective comparison
916 between one traditional algorithm and four deep-learning architectures. *PLoS One*. **15** (10),
917 e0230605 (2020).

918 70 Heinrich, L., Bennett, D., Ackerman, D., Park, W. Whole-cell organelle segmentation
919 in volume electron microscopy. *Nature*. **599** (7883), 141–146 (2021).

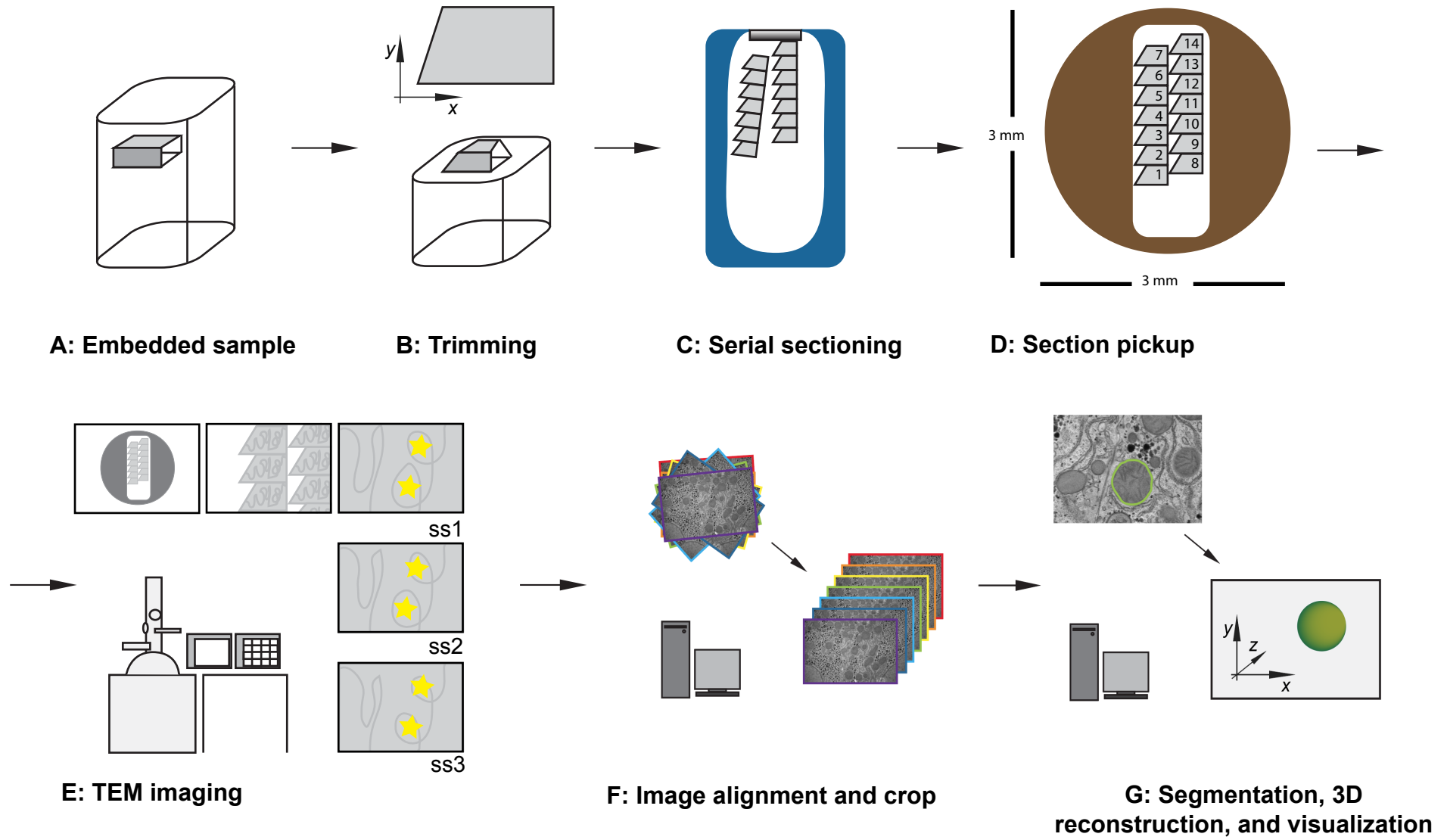
920 71 Kim, J. S., Greene, M. J., Zlateski, A., Lee, K. Space-time wiring specificity supports
921 direction selectivity in the retina. *Nature*. **509** (7500), 331–336 (2014).

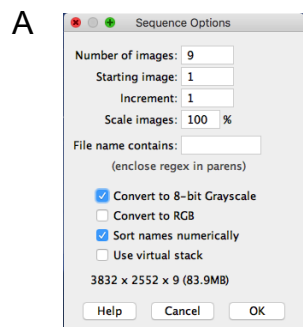
922 72 Spiers, H., Songhurst, H., Nightingale, L., de Folter, J. Deep learning for automatic
923 segmentation of the nuclear envelope in electron microscopy data, trained with volunteer
924 segmentations. *Traffic*. **22** (7), 240–253 (2021).

925 73 Hasan, N. M., Gupta, A., Polishchuk, E., Yu, C. H. Molecular events initiating exit of a
926 copper-transporting ATPase ATP7B from the trans-Golgi network. *The Journal of Biological*
927 *Chemistry*. **287** (43), 36041–36050 (2012).

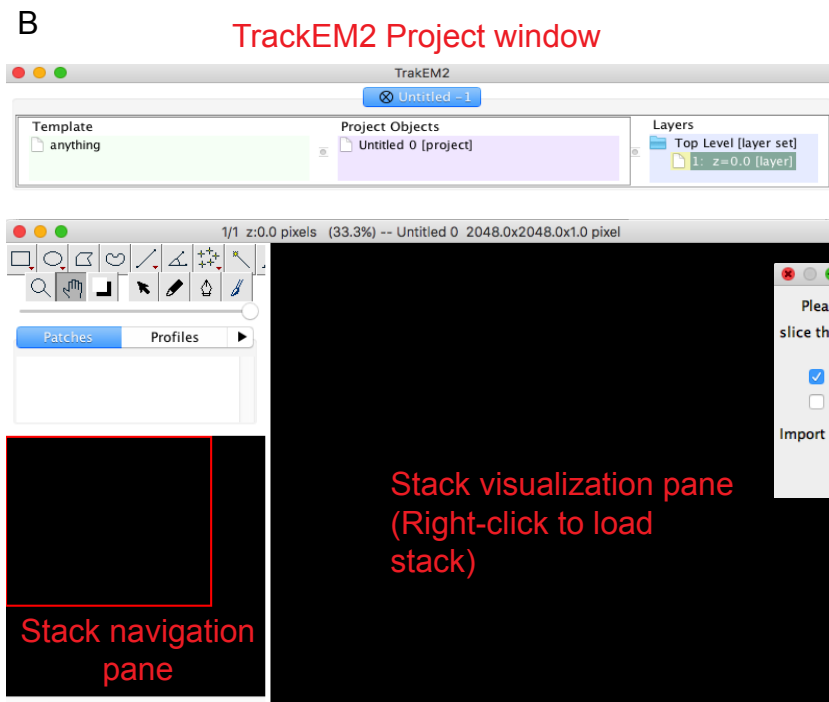
928 74 Stoeck, I. K., Lee, J. Y., Tabata, K., Romero-Brey, I. Hepatitis C virus replication
929 depends on endosomal cholesterol homeostasis. *The Journal of Virology*. **92** (1), e01196-17
930 (2018).

931 75 Ma, X., Qian, H., Chen, A., Ni, H. M., Ding, W. X. Perspectives on mitochondria-ER and
932 mitochondria-lipid droplet contact in hepatocytes and hepatic lipid metabolism. *Cells*. **10**
933 (9), 2273 (2021).
934
935

Figure 1

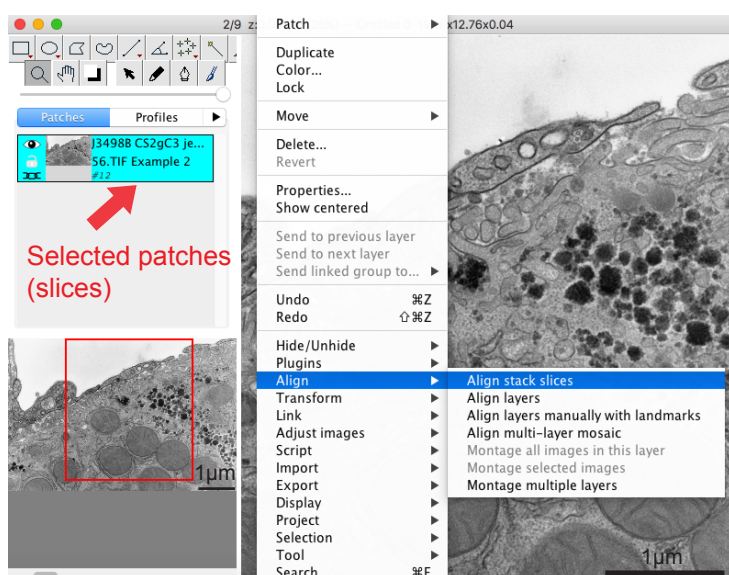


Stack Creation & Import to TrackEM2

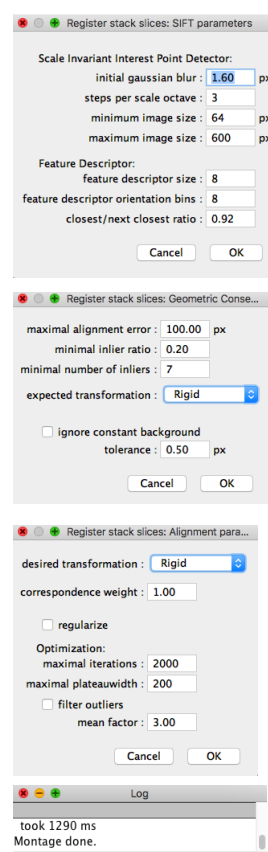


C

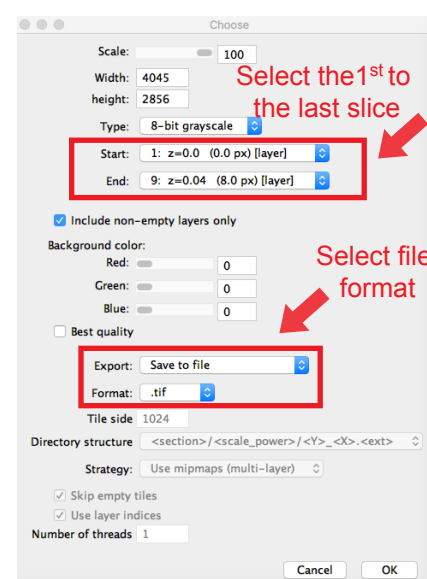
1. Check imported slices



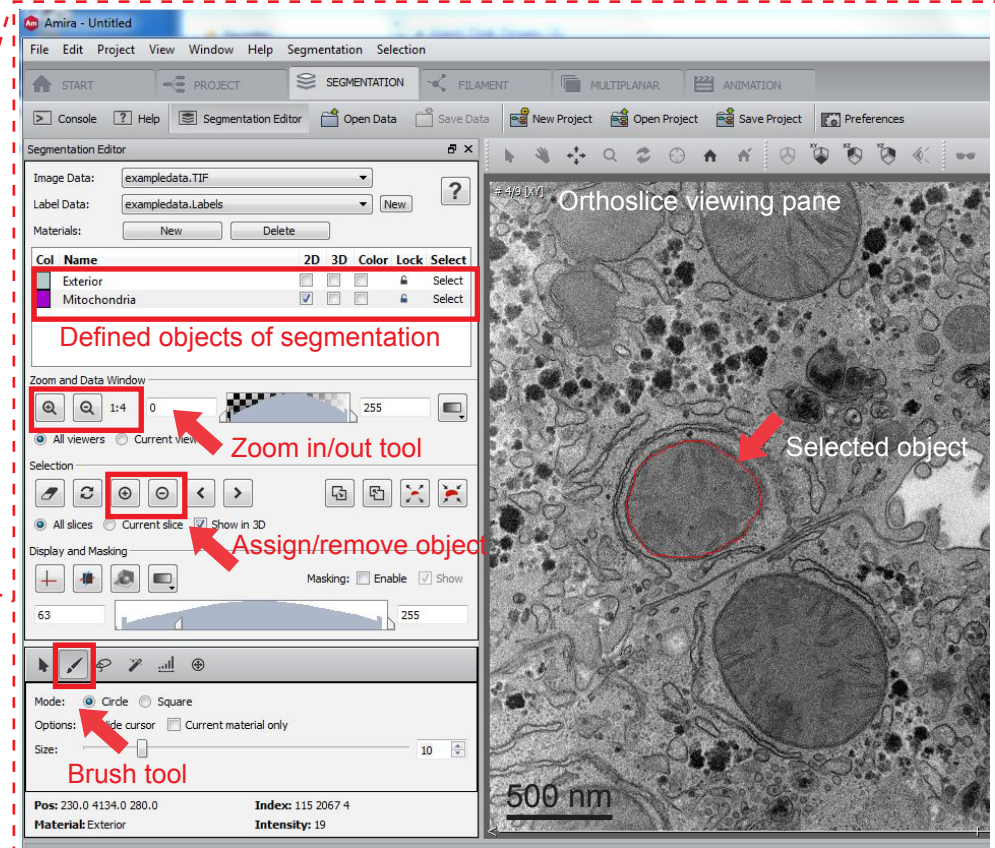
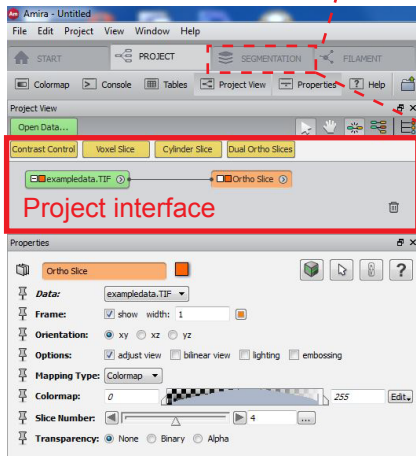
2. Set alignment parameter



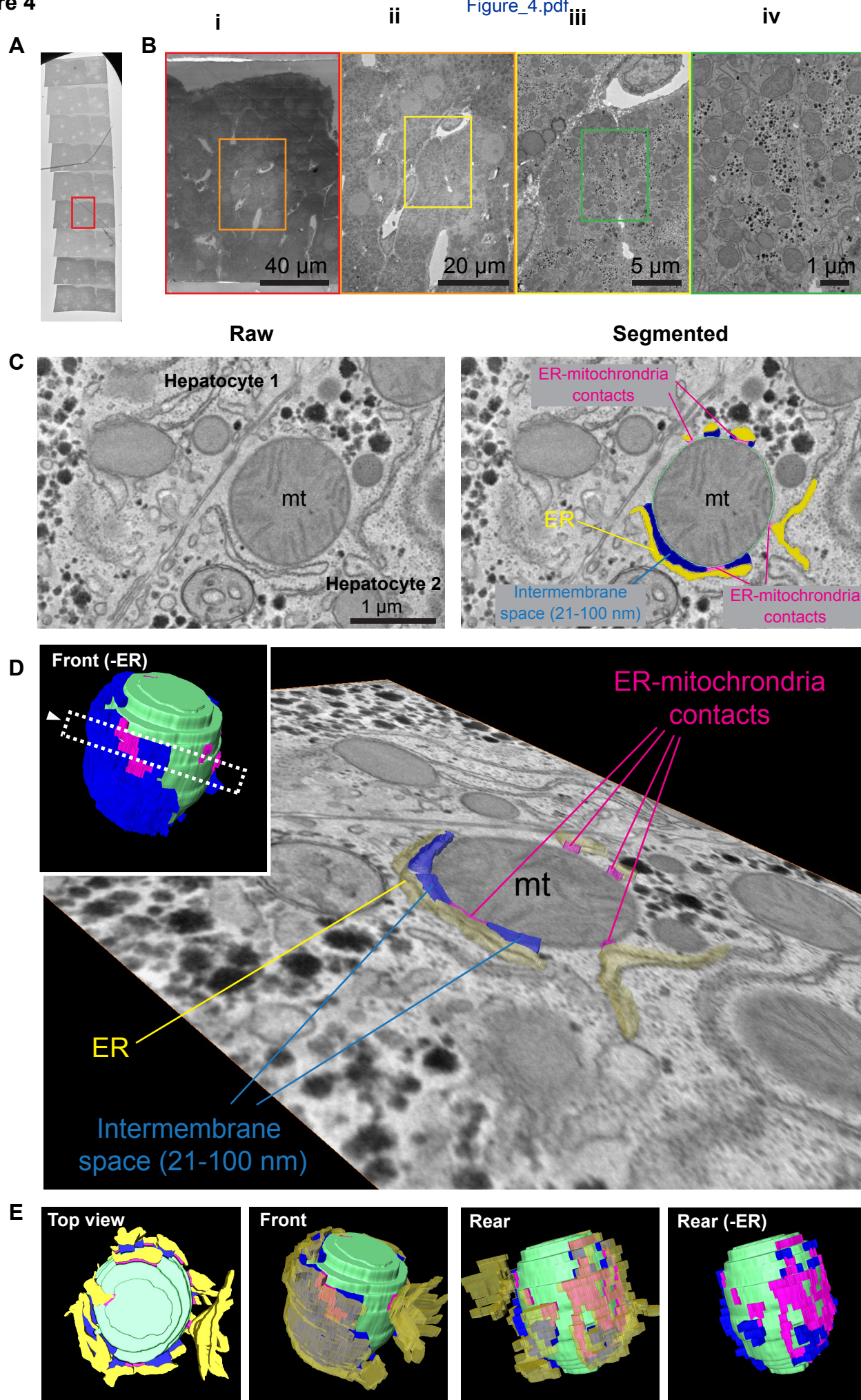
3. Save and export aligned stack



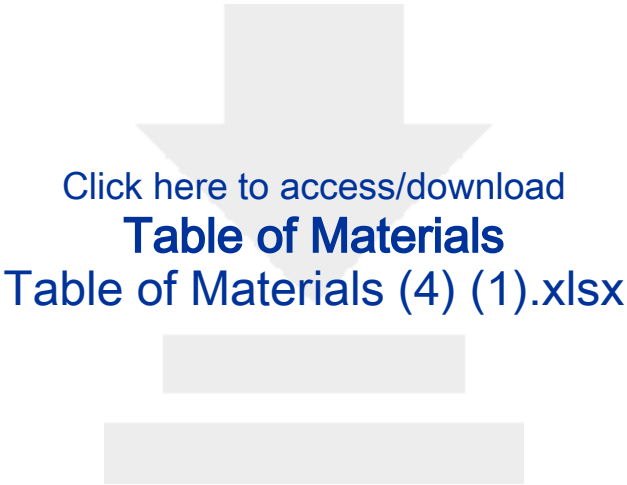
C



Segmentation Panel



Concerns	Serial Tomography	Serial Section TEM	FIB-SEM	SBF-SEM	Array Tomography
Lateral (x,y) resolution (Minimum px size)	0.5 nm	0.5 nm	2 nm	2 nm	2 nm
Axial (z) resolution (Minimum px depth)	1 nm	50 nm Limited to section thickness	4 nm	20 nm	50 nm Limited to section thickness
Volume ranges of data in typical applications	0.1 - 50 μm^3	10 - 250 μm^3	10 - 1 x 10 ⁴ μm^3	10 - 1 x 10 ¹² μm^3	10 - ∞ μm^3
Revisit or reimage of the samples	Possible	Possible	Not possible	Not possible	Possible
Cost of the equipment (instrument examples)	££ (200 kV TEM)	£ (120 kV TEM)	££ (FIB-SEM)	££ (SBF-SEM)	££ (SEM+AT)
Cost of equipment maintenance	££	£	££	££	£



Dear Editor,

Thank you giving us the opportunity to submit a revised draft of our manuscript titled “**3D Characterisation of Endoplasmic Reticulum-Organelle Membrane Contact Sites in Hepatocytes using Serial Section Transmission Electron**” [JoVE63496]. We appreciate the time and effort that you and the reviewers have dedicated. We are grateful for the constructive and insightful comments and we have been able to incorporate changes to accommodate most of the suggestions.

We have uploaded the revised version, with all changes accepted, as well as a tracked changes copy should you need it.

Below is a point-by-point response to the editorial and reviewers’ comments.

Editorial comments:

1. Please take this opportunity to thoroughly proofread the manuscript to ensure that there are no spelling or grammar issues.

Response: We have corrected all the spelling and grammar mistakes.

2. Please shorten the title along the lines of “3D Characterization of Inter-Organelle Contacts in Hepatocytes using Transmission Electron Microscopy”

Response: We have changed the title to “3D Characterisation of Inter-Organelle Contact Sites in Hepatocytes using Serial Section Electron Microscopy”

3. Please revise the text to avoid the use of any personal pronouns (e.g., "we", "you", "our", "your" etc.).

Response: We have excluded the use of all personal pronouns in the manuscript.

4. Please remove all commercial language from your manuscript and use generic terms instead. All commercial products should be sufficiently referenced in the Table of Materials (For example: TAAB, Devcon, etc.)

Response: All commercial terms have been removed and only included in the *Table of Materials*.

5. ml should be mL, µl should be µL, and minutes should be min throughout the manuscript. Please include a single space between the numeral and the unit, e.g., 24 h, 4 °C, etc.

Response: All units are following the correct SI/metric format now.

6. For in-text formatting, corresponding reference numbers should appear as numbered superscripts without brackets after the appropriate statement(s), but before the punctuation.

Response: All in text citations are now following the JoVE format.

7. Please revise the Introduction to also include the following:

a) A description of the context of the technique in the wider body of literature

b) Information to help readers to determine whether the method is appropriate for their application

Response: We have extended our paragraphs so that the key features of various volumetric EM techniques are discussed, and included a comparison table. This will help readers to decide which techniques are suitable for their application.

8. Lines 43-51: Please provide relevant citations.

Response: This section has been re-written in response to Reviewer 1’s comments, and we have included relevant citations, please see the last paragraph of the revised Introduction.

9. Please refrain from using bullets or dashes in the Protocol section.

Response: We have removed all bullets point in the Protocol section and have limited our use of dashes.

10. Please use a single line spacing between steps and sub steps of the protocol.

Response: Format changed accordingly.

11. Please add more details to your protocol steps. Please ensure you answer the “how” question, i.e., how is the step performed? Alternatively, add references to published material specifying how to perform the protocol action.

a. Step 1.2: how warm is the fixative (i.e., temperature) and what is its composition?

b. Steps 2.4-2.6: how many times is the washing in each of these steps repeated?

Response: We have included details for the fixative temperature and composition and the number of times the washing steps should be repeated.

12. Step 5.4: Please simplify the Protocol so that individual steps contain only 2-3 actions per step and a maximum of 4 sentences per step.

Response: The originally Step 5.4 has been simplified and broken down into new Step 5.4 and Step 5.5.

13. Step 7.1: Please cite the source of Amira. Please include the download/source links for the software/plugins used in this study in the Table of Materials.

Response: Done.

14. Line 423: please fix the typos (“?”) in tissue dimensions.

Response: Typos has been corrected, see representative results paragraph 1.

15. Panel 4D is not discussed in Results section. Please do.

Response: We have included the description for Figure 4D.

16. Figures 2-4: please include scale bars in all the microscope images.

Response: All microscope images now include a scale bar.

17. Figure 4: Please include the scale corresponding to the scale bars in panel B. Please also mention what the far-right image of panel E denotes.

Response: We have included the values for scale bars and labelled all the reconstructed 3D models.

18. Remove the embedded Table of Materials.

Response: A separate Table of Materials is provided in the modified manuscript.

19. As we are a methods journal, please revise the Discussion to also cover the following explicitly in detail in 3-6 paragraphs with citations:

Response: We have endeavoured to include these aspects in the following paragraphs.

a) Critical steps within the protocol

Response: Discussion paragraph 3 and 4

b) Any modifications and troubleshooting of the technique

Response: Discussion paragraph 3 and 4

c) Any limitations of the technique

Response: Discussion paragraph 2 and Overview table

d) The significance with respect to existing methods

Response: Discussion paragraph 2 and Overview table

e) Any future applications of the technique

Response: Discussion paragraph 1 and 7

20. Please revise the Table of Materials to include all the supplies (chemicals, reagents, equipment, consumables, software, etc.) used in this study.

Response: We have updated the Table of Materials accordingly

21. Please ensure that the references are numbered in the order of appearance and are formatted as the following: [Lastname, F.I., LastName, F.I., LastName, F.I. Article Title. Source. Volume (Issue), FirstPage – LastPage (YEAR).] For more than 5 authors, list only the first author then et al. Please expand journal names.

Response: The bibliography now follows the JoVE format.

Reviewers' comments:

Reviewer #1:

Manuscript Summary:

In the manuscript entitled '3D characterization of Endoplasmic Reticulum-Organellar Membrane contact sites in hepatocytes using serial section transmission electron microscopy, Burden et al propose a robust and efficient way to collect serial sections for electron microscopy and conduct quick 3D analysis of biological compartments of optimized volumes.

In the abstract, the author describes carefully the scientific context of their work and the advantageous reason for conducting serial section TEM to investigate 3D properties of dynamic and highly plastic biological sub-compartment such as the ER.

The proposed manuscript is highly detailed, close to a book chapter level, and nicely written so it's easy to read through and could become a bench protocol to any user with experience in the field.

Response: We thanks the reviewer for the kind and constructive comments.

Major Comments:

1. The title inspires a biology paper with the biological outcomes, while the content is focused on a methodology presentation. I would suggest transforming significantly the title to reflect more the actual purpose of the paper and avoid confusion of the readership.

Response: As this protocol was invited to be part of a special issue entitled “Emerging models and methods to investigate liver regeneration and disease”, we aimed to write a balance manuscript to include significant

details relating to both the method and the biology. However, we thank and appreciate your comments and as such have tried to modify the Abstract, Introduction and Discussion to also demonstrate the breadth of the application. With respect to the title, we have changed the title from “3D Characterisation of Endoplasmic Reticulum-Organelle Membrane Contact Sites in Hepatocytes using Serial Section Transmission Electron” to “3D Characterisation of Inter-Organelle Contact Sites in Hepatocytes using Serial Section Electron Microscopy” to hopefully broaden its readership and better reflect the protocols applications.

2. The same comment applies to the abstract (first half is about biology, second half starting line 27 about the method), and even more to the introduction (two paragraphs on biology, one on methodology that could be the actual abstract, no presentation on serial sectioning and existing literature).

Response: We agree with the reviewer and in light and agreement with comment 1, have revised the Abstract and Introduction to emphasize the methodological elements, including references to serial sectioning approaches, modifications and tips and tricks.

3. To me, this is the main limitation of this article so far: strong discrepancy between abstract/introduction and content.

Response. We agree with the reviewer’s comment so that we have revised the Abstract and Introduction so that the theme of this manuscript is more coherent.

4. The paper present no novelty in method nor in results, but has the quality of synthesizing several technical and software tools into one readable and detailed workflow.

I would empathize that the strong place of the biological topic could even drag away readers not from the biological field but with a great interest for the method that is applicable to a wide range of questions.

In the 'representative results' section, the structure is correctly presenting the outcome of the method. In the second paragraph, 431-432, I would suggest rephrasing in a way that the ER has been used as a case study to support the benefit of the method. It currently reads more to me as a bio paper on ER analysis (logical with the abstract but see comments above). The third paragraph used adequately the biological topic to illustrate the method.

Response: We thank the reviewer for the critical comments. We have changed the focus of the introduction and discussion, put more attention to the details for the serial sectioning technique and toned down the focus of our biological case study.

In the discussion, other 3D techniques are presented that are now spreading rapidly. I would suggest to find a way to illustrate the benefit of the authors' methods compared to other (FIB-SEM, 3View, Array Tomo) in regard to the 'volume of acquisition/speed of acquisition/equipment available at hand/cost/time to run the experiment/ease of the experiment/ease to analyse the results (maybe not all at once, but those elements are of interest). It would illustrate nicely the benefit of their approach and would help facility managers to guide their users towards one method of the other according to their project.

Maybe a reference to the first full eukaryotic cell imaged by electron tomography of a serial section would also be wise (Höög et al, dev cell).

Response: We have created an overview table giving a comparison of the different vEM techniques. This includes resolutions achievable, average volumes acquired, costs to purchase and costs to maintain, to help guide the readers depending upon their research needs. We have additionally included relevant references and reviews of the techniques. We did not extensively compare speed and ease of acquisition between the techniques, because this varies significantly depending upon the volume of data required, but have referenced this aspect in Discussion paragraph 2. We have included the beautiful Höög et al, reference.

Minor Comments:

1. What is the function of the Triton X-100? I am familiar with the use of Chloroform to spread and unfold sections, but I never used Triton, what advantage does it bring?

Response: We have included why the use of Triton X-100 is useful during sectioning and collection.

2. Line 250, paragraph 3.14, the authors mention the use of a ball-dropper. I am not familiar with this tool. A commercial reference of a picture could be of interest

Response: We have changed the text to better reflect the catalogue name of “Glass applicator rod” and included its ordering details in the Table of Materials.

3. Nice serial sections are easier to collect with highly parallel bloc faces top and bottom. This can be achieved using a trimming cryo-knife, but then the very sharp and clean bloc face is causing difficulties to get attaching ribbons. Trimming with razor blades is less clean and helps to get sections attached, but not always. To get nice serial sections, some glue or wax could be deposited below the bloc face to help keep the ribbons together.

There is no mention of it, and I think it could be of interest to the readership. Some literature already mentions and discusses that (methods in cell biology and journal of microscopy to my memory).

Response: In the protocol section we have described the use of a razor blade and included the use of trimming diamond knives as an alternative option. We have also included the use of contact cement to aid ribbon stability as an alternative. We have also briefly mentioned this in the Discussion paragraph 4 of the revised manuscript.

4. The protocols to use trackEM2 and Amira are nicely described and will satisfy many users.

Response: We thank the reviewer for the kind comment.

Reviewer #2 comments:

The manuscript by Chung et al presents a well-detailed protocol based on Serial Section Transmission Electron Microscopy that can be used to identify spatial interactions between organelles, including contact sites.

Overall, I found the manuscript interesting and the protocol very clear. I think that it would be nice to include a video showing the 3D reconstruction of the example shown in Figure 4 so as to appreciate better the power of this technique. (Unless such a video will be shown as part of the video of the technique)

Response: We thank the reviewer regarding the positive comments. We are happy to include the 3D model reconstruction as part of the protocol video. However, if the video time is limited, we are also happy to provide a separate video.

Minor Comments:

1. S18, omit "as"

2. S52, "types" instead of type

Response: The above grammar mistakes have been fixed.

3. Section 1.5, specify composition of fix

Response: We have specified the composition of the fixative.

4. Section 1.6, how to select regions of interest?

Response: How to select a region of interest is very research-question dependent, however we have provided details of some general considerations when selecting a region of interest, see Note in 1.6 of the revised manuscript.

5. Section 2.9 is same as section 2.10

Response: Step 2.10 is a repeated step. We have modified the sentence so that it is clearer in the protocol.

6. S218, is Triton used neat?

Response: Apologies, we have now included the concentration of 0.1% Triton X-100 in 3.7 and 3.8 of the revised manuscript protocol section.

7. S448, replace "have" with were

Response: Grammar mistake has been corrected.

8. S449-2450, Sentence starting with "Figure 4E..." is hard to understand. Figure 4, it may work better to make the lines pointing to the contact regions thinner because as it is the small areas of contact are difficult to discern when the fat lines hit them

Response: The corresponding sentence has been rewritten. We have rescaled the lines that annotate the different intermembrane space(s).

Reviewer #3 comments:

Manuscript Summary: The authors describe in detail a protocol to perform Serial Section Transmission Electron Microscopy on liver tissue, to obtain 3D EM information that allows for characterization of ER - organelle contact sites. The structure of the article follows the logical order of the experimental procedures, starting with specimen fixation and preparation, over procedures for sample mounting, image acquisition, image restoration and segmentation, and 3D reconstruction. Each and every step of the workflow has been extremely well described and based on the written text, scientists with prior know-how on electron microscopy techniques will definitely be able to use this documentation as a source of reference to execute the described protocol. The figures that have been provided show essential information and the paragraphs that have been indicated to use for video documentation are spots on because these are steps in the workflow that would require visual demonstration in order to be able to carry out the protocol. I am in absolute favor to publish this work with only very minor suggestions for additions.

Response: We thank the reviewer for the kind comments. We have addressed the minor concerns and have provided more details on other volumetric EM techniques in the text.

Minor Comments:

1. In the discussion the authors elaborate on liver sample preservation by whole liver perfusion or liver wedge needle perfusion. In the protocol, the latter has been described. I would suggest that this procedure would also be included in the video material, because I'm convinced this is valuable to anyone that would like to perform any EM technique on liver tissue.

Response: We agree with the reviewer that for liver researchers a needle perfusion video might be helpful however it will depend on the availability of the mice at the timing of filming. If it is possible, we will endeavour to include it.

2. Please provide info on PO in your table of Materials.

Response: We have now included the ordering details of PO in the table of materials of the revised manuscript.

3. Please check the spelling of Triton X-100. In the current version of the manuscript this is not consistent throughout the text.

Response: We have made the spelling consistent throughout the whole manuscript.

4. Line 423: the symbol for micron is not correctly displayed.

Response: Apologies the typos has been fixed, see Representative results paragraph1

5. Step 6.4: What is the original bit depth? Can the authors elaborate on why they convert images to 8-bit. In view of the processing steps that are used later in the protocol there is no downside to converting images to 8-bit formats. However, if anyone was to apply (semi-)automated segmentation in later steps, it may be beneficial to not alter the original bit depth.

Response: We agree with the reviewer. Our microscope originally produces 16 bit depth images, but are incorrectly read by software packages as 12 bit. We routinely convert for 3D reconstruction to 8 bit as it reduces the data size without compromising resolution to aid data processing and allows easier inter-software handling. We have included the reasons why we recommend converting images to 8-bit as a prerequisite for other data handling steps, see note in protocol 6.4.

Yours sincerely

A handwritten signature in black ink, reading 'Jemima Burden'. The signature is fluid and cursive, with a long horizontal stroke at the end.

Jemima Burden